

Laser cladding of Ti-6Al-4V alloy with vanadium carbide particles

El-Labban, H.F.^a, Mahmoud, E.R.I.^{a,*}, Al-Wadai, H.^a

^aFaculty of Engineering, King Khalid University, Abha, Saudi Arabia

ABSTRACT

The tribological properties of Ti-6Al-4V alloy are generally poor. This study was an attempt to produce a hardened surface layer on this alloy for longer service life during severe wear conditions. For this purpose, laser surface cladding of this alloy with vanadium carbide (VC) powder was performed using a YAG Fiber laser at power strengths of 1000 W, 1500 W, and 2000 W and a travelling speed of 4 mm/s. Surface clad layers of Ti-6Al-4V alloy metal matrix composite reinforced with VC particles were produced on the substrate under all processing conditions. The size of the cladding layer was increased by increasing the processing power. The cladding layer was well bonded to the substrate, especially at higher processing powers. The VC particles were homogeneously distributed within the cladding layer at processing powers of 2000 W and 1500 W, whilst it showed some clusters at a power of 1000 W. Some of the VC particles were melted and re-solidified as fine long dendritic structures during the laser treatment. The cladding layer produced under all processing conditions exhibits remarkable improvement of hardness and wear resistance (almost twice). As the processing powers decreased, the surface of the cladding layers showed higher hardness. The cladding layer also showed improved corrosion resistance.

© 2014 PEI, University of Maribor. All rights reserved.

ARTICLE INFO

Keywords:

Laser cladding
Ti-6Al-4V alloy
VC powder
Surface microhardness
Wear and corrosion resistance

*Corresponding author:

emahoud@kku.edu.sa
(Mahmoud, E.R.I.)

Article history:

Received 2 August 2014
Revised 29 October 2014
Accepted 10 November 2014

1. Introduction

Titanium and its alloys are used for manufacturing of some components in automobile, aerospace, marine, medicine, chemical and energy industries, due to their improved properties such as high strength-to-weight ratio, excellent corrosion resistance, high temperature strength, high Young's modulus and high cycle fatigue properties [1-3]. Ti-6Al-4V alloy is considered the most used alloy in these applications. However, the uses of this alloy in the severe environments, where the wear is the main failure mode, are limited due to its poor wear resistance [4]. To overcome this problem, it is necessary to improve the surface wear resistance. Many different traditional surface modifications such as surface hardening [5] and surface cladding [6, 7] are applied to improve wear and erosion characteristics of the surfaces of Ti alloys. Various techniques such as thermal spraying [8], plasma spraying [9], traditional arc welding and focused energy technologies like electron beam [10] and laser [11-13] have been employed. The excessive energy input from the traditional welding processes such as shielded metal arc welding or even gas tungsten arc welding may cause some undesirable distortion and residual thermal stresses which may cause cracks in the hardened layer [6, 7]. Laser surfacing has been suggested as a potential technique to produce a hard surface layer of Ti alloys for a number of reasons. The most important one arises from the fact that laser beam has rapid heating and cooling, which

can easily produce special types of microstructure with novel properties that cannot be produced by other conventional processing technique [14, 15]. Generally, the obtained microstructure in the laser treated area is dependent on the heating and cooling cycles that take place during the process, which in consequence depends on the laser parameters [16]. Other merits of the laser surfacing are to produce a hard layer with low dilution and deformation, relative cleanliness, lack of quenching medium and limited grain growth during the heating [11].

Laser cladding process is considered one of the laser surfacing techniques that can produce Ti alloy-based composites clad layer where hard particles such as carbides, borides, and nitrides are used to reinforce the Ti alloy [17]. In this case, the wear properties can be improved by the combination of embedded hard carbide particles and the rapid heating and cooling which forms hard structure matrix. The widely used carbide particles as reinforcement are titanium carbide (TiC) and vanadium carbide (VC). VC possess many favorable properties, such as high hardness (2460-3150 HV_{0.05}) [18], high melting temperature (2830 °C) [19], low heat conductivity [20], certain plasticity, and good wettability to metal bonding. Moreover, VC has a low-friction coefficient [21]. Besides, when VC is used in high temperatures, it is oxidized to vanadium oxide (V₂O₅), which is characterized by self-lubrication performance [22, 23]. This advantageous combination can create a protective coating layer on the surface of the composite material with enhanced resistance against thermal, corrosion and mechanical wear [24, 25].

Thus, in the present study, we aim to investigate the effects of main laser parameters and rapid solidification on the microstructure, hardness and wear behaviour of Ti-6Al-4V alloy surface clad by VC powder. Microstructural changes in the build-up, melted, and heat affected zones are examined in details.

2. Experimental work

Specimens of Ti-6Al-4V alloy were used as substrate with dimensions of 100 mm × 50 mm × 3 mm. The surfaces of specimens were cleaned and the oxides were removed by grinding using emery papers. In order to avoid the oxidation of the strip during the treatment, argon with the flowing rate of 15 L/min was used as a shielding gas during and after the treatment. The cladding treatment was carried out using VC powder with 40-50 μm particle size as a cladding material and YAG Fiber laser (Ytterbium laser system, YLS-3000 SM, 3 kW). The powder was pre-placed on the top surface of the strip with 0.5 mm height and then emitted by laser beam. The treatments were conducted at different laser power strengths of 1000 W, 1500 W, and 2000 W, and at fixed travelling speed of 4 mm/s. The process was conducted at a defocusing distance (D_f) of 24 mm. The microstructures of the coated layer and substrates were investigated using optical microscope and scanning electron microscope equipped with EDS (Energy-dispersive X-ray spectroscopy) analyser. The micro-Vickers hardness in the coated layer cross-section and the substrate were measured with an indentation load of 9.8 N and loading time of 15 s at room temperature. The wear behaviour of the laser clad zone was evaluated using a pin-on-disk dry sliding wear tester in air at room temperatures. A stationary sample with a diameter of 2.5 mm was slid against a rotating disk with a rotational speed of 265 rpm for 15 min. The tests were carried out at a fixed load of 2 kg applied to the pin. Before the test, all the specimens were ground on emery paper up to # 600 to get smooth and flattened surface. The specimens were weighted before and after the test with a sensitive electronic balance with an accuracy of 0.001 g. The differences in average weight before and after the wear test were measured and accounted. Three specimens of each condition were chosen for wear tests. The untreated base metal was selected as the reference material for the wear test. The corrosion behavior of the substrate and the cladding layer were evaluated by the corrosion current density and the corrosion potential obtained from polarization curves in a 3 wt. % NaCl solution at room temperature with an IM-6 electrochemical workstation. The scanning potential can be in the range of -1.0 V to +2 V, and the scanning rate was 5 mV/s.

3. Results and discussion

3.1 Macro and micro-structure analysis

Fig. 1 shows the macrographs of the cross-sections of the surface laser treated layer at different processing powers. The treated layers in all conditions appeared as nearly half moon shape inside the Ti alloy substrate. This is may be due to the higher defocusing distance that penetrate the heat into deeper areas and increase the dilution of the cladding materials with the substrate. It was clear from these figures that the area of the cladding layer is in direct proportion to the laser power. At laser power of 2000 W, the cladding layer appeared as a deeper complete half moon above the substrate, while it appears as a narrow band at laser power of 1000 W. The dimensions of laser treated zones were 2.99 mm width and 0.52 mm depth for 1000 W, 3.05 mm width and 0.61 mm depth for 1500 W, and 3.1 mm width and 0.73 mm depth for 2000 W. This is due to the more heat input that produced at higher powers which melts the cladding materials together with more areas from the substrate. The microstructures of the cladding layer treated by power of 2000 W are shown in Figs. 2 and 4. Many (white color) fine long dendrites with short secondary arms were precipitated inside the Ti alloy as clearly shown in Fig. 2. EDS demonstrated that these dendrites were VC, as shown in Fig. 3(b), while the matrix was Ti alloy substrate, Fig. 3(a). This means that a surface composite consisted of Ti alloy reinforced with VC dendrites was produced in the clad layer. In addition, the dendrite morphology of the high melting point VC particles means that they were melted and then solidified during the laser processing. As it is well known that laser technology is characterized by a high energy density and ceramics have a much higher capability to absorb laser energy than metals [26]. Therefore, VC particles were melted (or partially melted) in spite of its extremely high melting point, and then solidified by the self-quenching effect of the very high cooling rate after laser surface treatment.

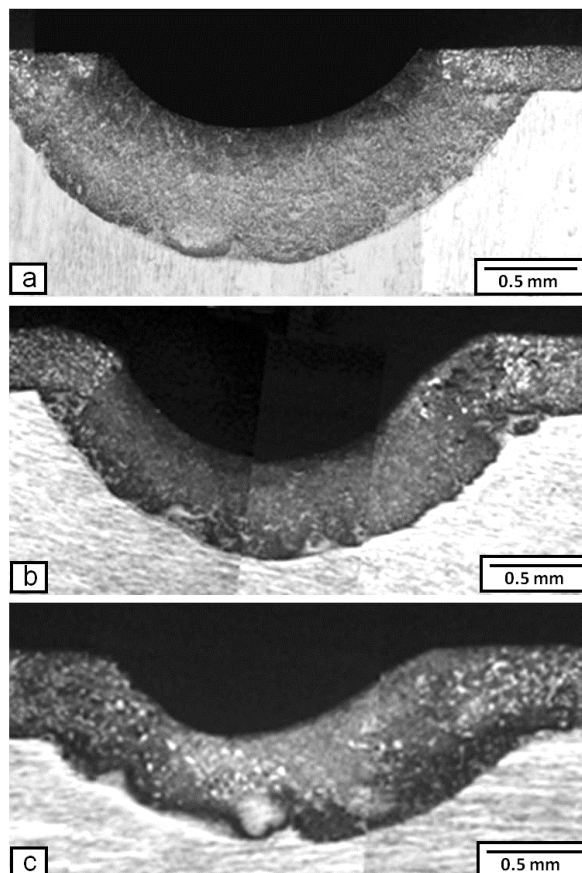


Fig. 1 Macro-views of the cross-sections of the surface laser cladding layer at different processing powers of 2000 W, 1500 W, and 1000 W

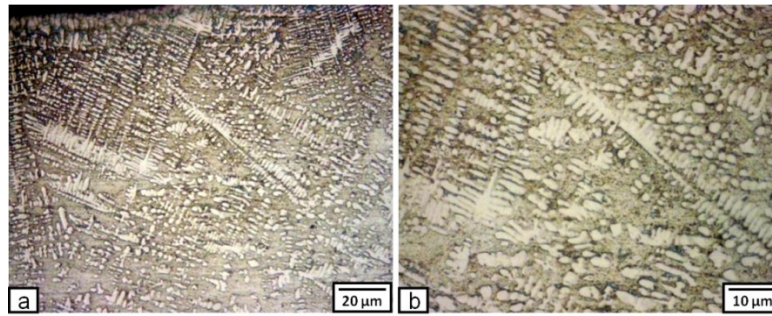


Fig. 2 Micrographs of the top portion of the laser cladding layer near the free surface produced by processing power of 2000 W

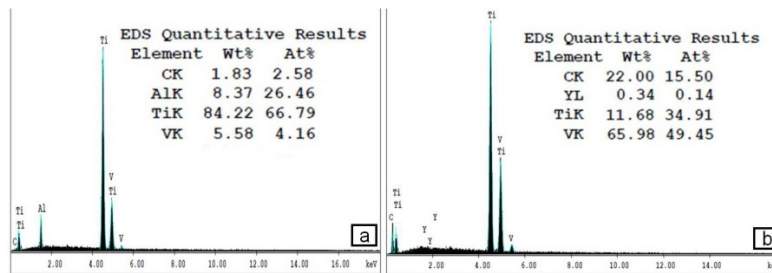


Fig. 3 EDS analysis of: (a) matrix, and (b) dendritic structure that appeared in the cladding layer produced at processing power of 2000 W

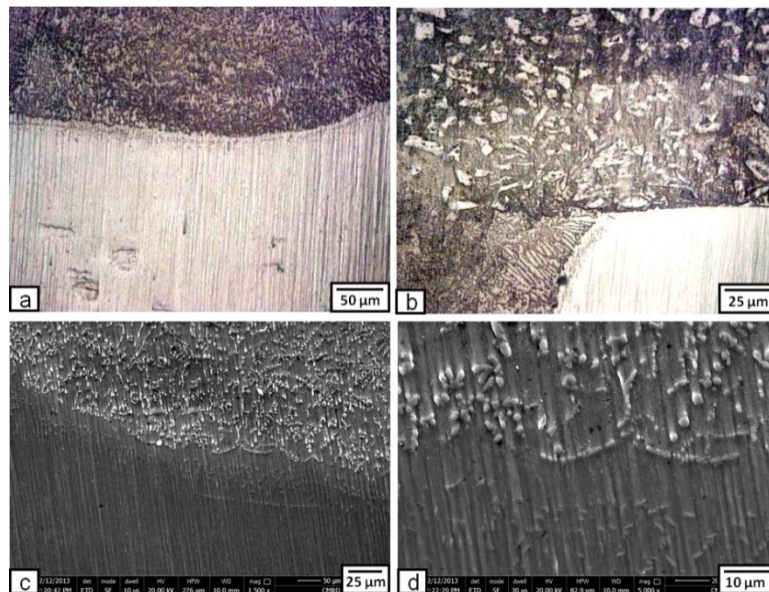


Fig. 4 Micrographs of the lower portion of the laser cladding layer produced by processing power of 2000 W showing the interface with the substrate

By going down through the cladding layer, near the interface, some fine VC particles are appeared distributed homogenously inside the Ti alloy matrix as shown in Fig. 4. In this area, the higher heat input melts the course VC particles. The relatively lower cooling rate at this embedded area was not fast enough to form VC dendrites. So, it appeared as fine VC particles. It is obviously to note here that the cladding layer was tightly bonded to the substrate without any defects as shown in Fig. 4.

At processing power of 1500 W, the amounts of VC dendrites are reduced and it concentrates at the top portion of the cladding layer (near the free surface) as shown in Figs. 5(a) and 5(b). The VC morphology is appeared as some dendrites mixed with particles. At the lower portion of

the cladding layer (near the interface), the VC particles appeared as their original coarse particles shape, as clearly shown in Figs. 5(c) and 5(d). The heat generated is not enough to melt most of the added VC particles. Most of the VC dendrites are concentrated at the top center of the cladding layer where the heat is concentrated.

When the laser processing power was reduced to 1000 W, the generated heat is not enough to melt the added VC particles. There was almost no dendritic VC morphology in the cladding layer produced at this condition as shown in Fig. 6. Moreover, the VC particles accumulated in clusters as shown in Fig. 6(c). The lower heat input at this condition reduces the dilution process of the VC particles in the Ti alloy matrix. This causes that the VC particles to concentrate in small area in their original shape.

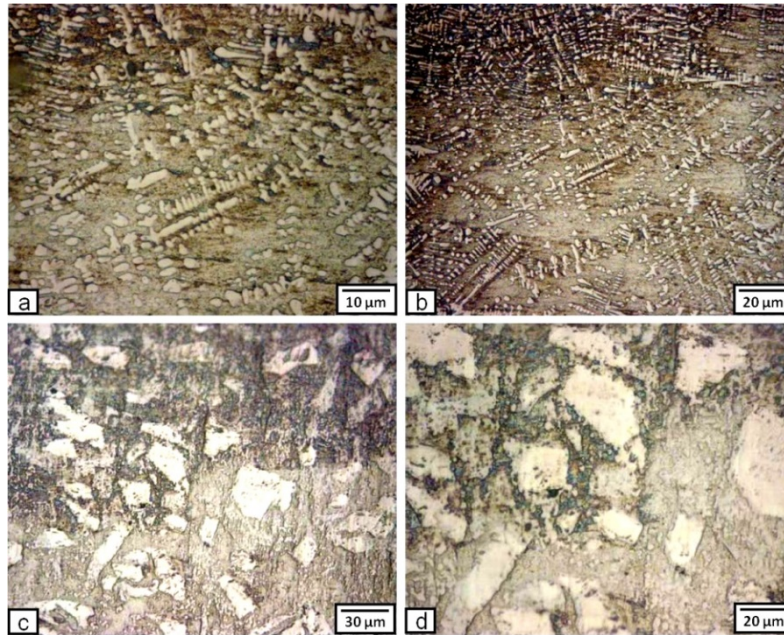


Fig. 5 Micrographs of the laser cladding layer produced by processing power of 1500 W: (a) and (b) – top portion near the free surface, (c) and (d) – lower portion

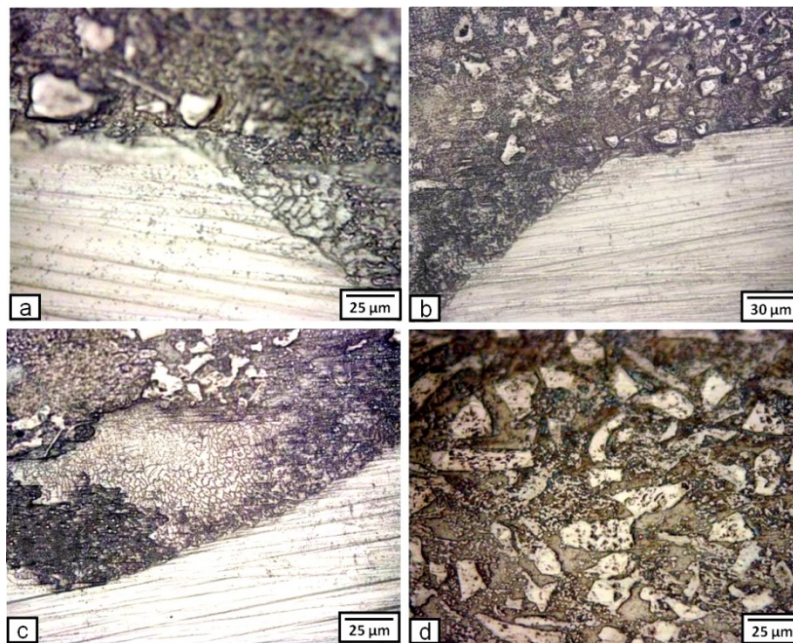


Fig. 6 Micrographs of the laser cladding layer produced by processing power of 1000 W: (a) – right side of the cladding layer, (b) – left side, (c) – lower center, (d) – center of the cladding layer

3.2 Surface and subsurface microhardness evaluation

Fig. 7 shows the hardness distribution along the depth direction of the laser-cladded areas at different powers. The substrate has an average microhardness value of approximately 360 HV. At all condition, high microhardness values (almost twice as the substrate) were obtained at the surface and a certain subsurface layer and decreased towards the substrate. This is due to the presence of hard VC particles with a great amount in these areas.

These results also indicate that the increase in processing power cause a decrease in the free surface hardness improvement and an increase in the hardened zone depth. The decrease in processing power decreases the amount of the heat input and consequently the dilution is decreased. As a result, the volume fractions of VC in the cladded layer are increased. This represents a main reason for the high hardness values resulted in case of the low processing power. Conversely, the increase of processing power increases the heat input and consequently the dilution is increased. As a result, the volume fractions of unmelted VC in the cladded layer are decreased. Moreover, during the re-solidification, some carbon came from the melted VC particles can be pushed by the solidification front due to it has low solubility in Ti [20, 21]. For that reason, the percentage of carbon in this region can be increased. This can be represents one of the main reasons for the high hardness at this region.

The hardness distributions at powers of 2000 W and 1500 W showed almost homogenous trend, which that at power of 1000 W showed inhomogeneous distribution. This may be due to the homogeneity of the VC particles inside the cladding layer, which confirm the microstructure analysis.

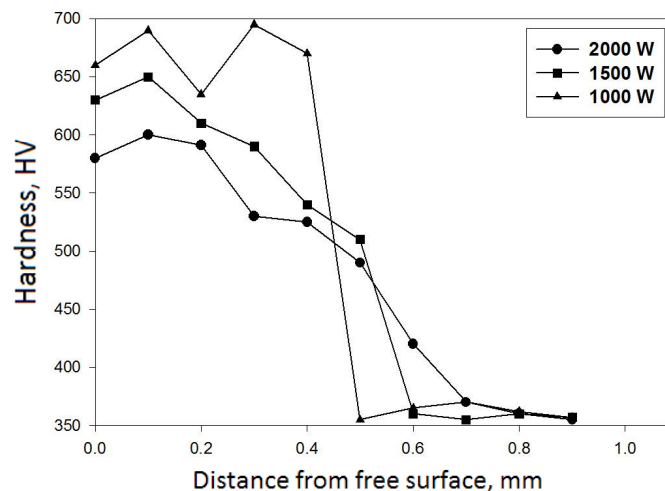


Fig. 7 Microhardness profiles through the depth of the laser treated zone obtained at different laser powers

3.3. Wear rate of the developed surface layer

The wear rates were calculated for the cladded layer and the substrate material as described in the experimental work. From Fig. 8 it is clear that the addition of VC powder on the Ti alloy substrate with the aid of laser improved the overall wear resistance of the MMC produced in the cladding zone on the surface. The three conditions of 2000 W, 1500 W, and 1000 W processing powers gave high reduction in wear rate. Generally, the improved wear resistance in the laser cladded zone can be mainly attributed to the higher hardness of this zone due to: i) the presence of VC in the form of refined particles and dendrites, ii) the carbon diffusion in the matrix and iii) the strong interface bonding between the Ti alloy matrix and the VC reinforcement. The hard reinforcing phase (VC) act as load-bearing compounds and resist the plastic deformation of the matrix phase. With the increase of power, the volume fraction of unmelted VC was decreased (due to the increase of dilution) and as a result the improvements in hardness and the wear resistance of the cladded zone were decreased. In the same time, the non-homogeneous distribu-

tion of VC particles inside the cladding layer at power of 1000 W increases the weight loss, and in consequence, reduces the wear resistance.

Regarding the corrosion resistance evaluation, the sample treated at processing power of 1500 W was chosen due to that it gave the best results regarding the dimensions, microstructure, hardness, and wear resistance of the resulted zone. Fig. 9 shows the polarization curves of Ti alloy substrate and the treated layer. From this figure, it is clear that the corrosion potential of the treated sample was shifted to more positive than that of the Ti alloy substrate. Also, the corrosion current of the treated layer showed lower values than that of the Ti alloy substrate. It is well known that when the potential is increased and the current is decreased, the polarization resistance is increased and the material show improved corrosion resistance. Thus, it is clearly evident that the laser melting of Ti alloy had a positive influence on its the corrosion behavior.

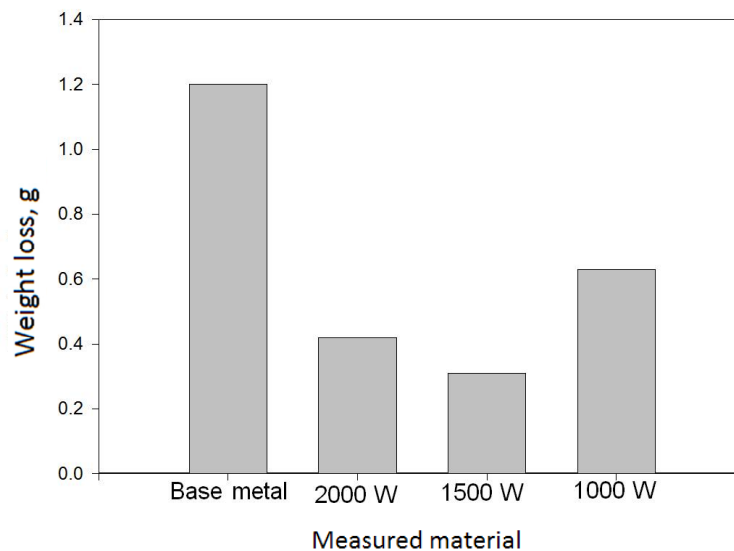


Fig. 8 Wear weight losses of untreated and laser cladde specimens with different laser powers

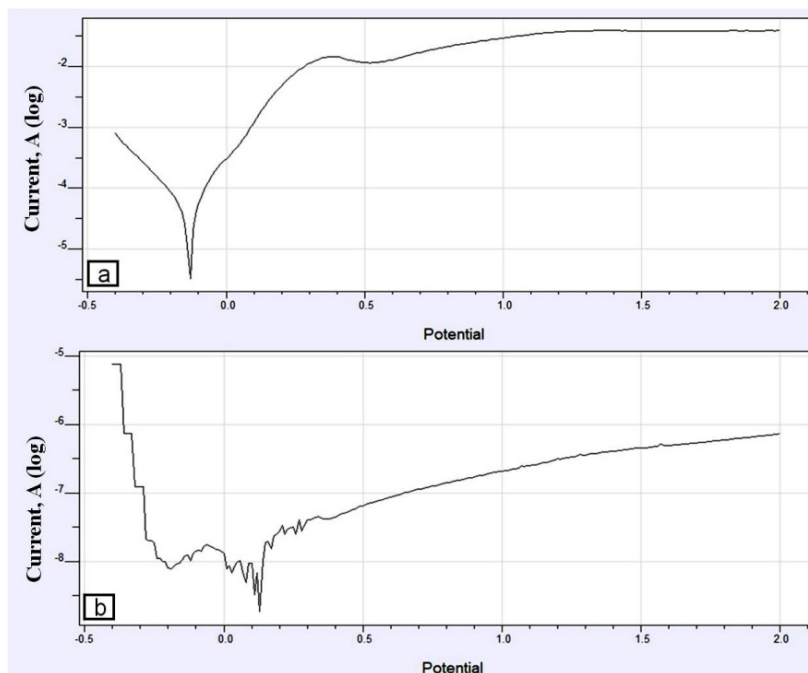


Fig. 9 Polarization curves of the substrate (a), and the cladding layer produced with processing power of 1500 W (b)

4. Conclusion

The surface of Ti-6Al-4V alloy was treated by laser cladding in argon atmosphere at processing powers of 2000 W, 1500 W, 1000 W, and fixed travelling speed of 4 mm/s. For this purpose, the YAG Fiber laser and VC powder as a cladding material with 30-40 μm particle size were used. The treated specimens were investigated in macro and microscopically scale using optical and scanning electron microscope. Surface and subsurface hardness, and wear and corrosion resistances were evaluated. The results of this work led to the following conclusions:

- Surface clad layers of Ti-6Al-4V alloy metal matrix composite reinforced with VC particles were produced on Ti-6Al-4V alloy at all processing conditions. The size of the cladding layer is increased by increasing the processing power. The cladding layer was well bonded to the substrate, especially at higher processing powers.
- The VC particles were homogeneously distributed within the cladding layer at processing powers of 2000 W and 1500 W, while it shows some clusters at power of 1000 W.
- Some of the VC particles were melted and re-solidified as fine long dendritic structure during the laser treatment.
- The cladding layer produced at all processing conditions resulted in remarkably improvement of hardness and wear resistance (almost twice). As the processing powers decreased, the surface of the cladding layers showed higher hardness. Higher laser power leads to a deeper hardened zone.
- The laser treated layer show improved corrosion resistance.
- The application of Ti-6Al-4V alloy can be widened by this surface treatment to include severe and harsh environment. Moreover, it can prolong their service life.

Acknowledgement

This work was supported by the King Abdel-Aziz City of Science and Technology (KACST) through the Science and Technology Center at King Khalid University (KKU), Project No. (10-ENE1161-07). The authors thank both KACST and KKU for their financial support. Special thanks to Prof. Ahmed Tahir, Vice President of KKU and Prof. Abdullah Al-Sehemi, Head of the Scientific Research at KKU for their support.

References

- [1] Ochonogor, O.F., Meacock, C., Abdulwahab, M., Pityana, S., Popoola, A.P.I. (2012). Effects of Ti and TiC ceramic powder on laser-clad Ti-6Al-4V in situ intermetallic composite, *Applied Surface Science*, Vol. 263, 591-596, doi: [10.1016/j.apsusc.2012.09.114](https://doi.org/10.1016/j.apsusc.2012.09.114).
- [2] Lin, Y.-C., Lin, Y.-C. (2011). Microstructure and tribological performance of Ti-6Al-4V cladding with SiC powder, *Surface and Coatings Technology*, Vol. 205, No. 23-24, 5400-5405, doi: [10.1016/j.surfcoat.2011.06.001](https://doi.org/10.1016/j.surfcoat.2011.06.001).
- [3] Mahamood, R.M., Akinlabi, E.T., Shukla, M., Pityana, S. (2013). Scanning velocity influence on microstructure, microhardness and wear resistance performance of laser deposited Ti6Al4V/TiC composite, *Materials and Design*, Vol. 50, 656-666, doi: [10.1016/j.matdes.2013.03.049](https://doi.org/10.1016/j.matdes.2013.03.049).
- [4] Tian, Y.S., Chen, C.Z., Li, S.T., Huo, Q.H. (2005). Research progress on laser surface modification of titanium alloys, *Applied Surface Science*, Vol. 242, No. 1-2, 177-184, doi: [10.1016/j.apsusc.2004.08.011](https://doi.org/10.1016/j.apsusc.2004.08.011).
- [5] Alabeedi, K.F., Abboud, J.H., Benyounis, K.Y. (2009). Microstructure and erosion resistance enhancement of nodular cast iron by laser melting, *Wear*, Vol. 266, No. 9-10, 925-933, doi: [10.1016/j.wear.2008.12.015](https://doi.org/10.1016/j.wear.2008.12.015).
- [6] Heydarzadeh Sohi, M., Ebrahimi, M., Ghasemi, H.M., Shahripour, A. (2012). Microstructural study of surface melted and chromium surface alloyed ductile iron, *Applied Surface Science*, Vol. 258, No. 19, 7348-7353, doi: [10.1016/j.apsusc.2012.04.014](https://doi.org/10.1016/j.apsusc.2012.04.014).
- [7] Benyounis, K.Y., Fakron, O.M.A., Abboud, J.H., Olabi, A.G., Hashmi, M.J.S. (2005). Surface melting of nodular cast iron by Nd-YAG laser and TIG, *Journal of Materials Processing Technology*, Vol. 170, No. 1-2, 127-132, doi: [10.1016/j.jmatprotec.2005.04.108](https://doi.org/10.1016/j.jmatprotec.2005.04.108).
- [8] Vamsi Krishna, B., Misra, V.N., Mukherjee, P.S., Sharma, P. (2002). Microstructure and properties of flame sprayed tungsten carbide coatings, *International Journal of Refractory Metals and Hard Materials*, Vol. 20, No. 5-6, 355-374, doi: [10.1016/S0263-4368\(02\)00073-2](https://doi.org/10.1016/S0263-4368(02)00073-2).
- [9] Hua, G., Huang, Y., Zhao, J., Wang, L., Tian, Z., Zhang, J., Zhang, Y. (2004). Plasma-sprayed ceramic coating by laser cladding of Al₂O₃ nano-particles, *The Chinese Journal of Nonferrous Metals*, Vol. 14, No. 2, 199-203.

- [10] Zenker, R., Buchwalder, A., Rüttrich, K., Griesbach, W., Nagel, K. (2013). First results of a new duplex surface treatment for cast iron: electron beam remelting and plasma nitriding, *Surface and Coatings Technology*, Vol. 236, 58-62, doi: [10.1016/j.surfcoat.2013.06.118](https://doi.org/10.1016/j.surfcoat.2013.06.118).
- [11] Zhang, W.P., Liu, S. (2005). Microstructure of Fe-Ti-B composite coating prepared by laser cladding, *The Chinese Journal of Nonferrous Metals*, Vol. 15, No. 4, 558-564.
- [12] Tian, Y.S., Chen, C.Z., Wang, D.Y., Wang, Z.L. (2004). Study on microstructures and mechanical properties of in-situ formed multiphase coatings produced by laser cladding of titanium alloy with silicon and graphite powders, *Chinese Journal of Lasers*, Vol. 31, No. 7, 879-882.
- [13] Chehrghani, A., Torkamany, M.J., Hamed, M.J., Sabbaghzadeh, J. (2012). Numerical modeling and experimental investigation of TiC formation on titanium surface pre-coated by graphite under pulsed laser irradiation, *Applied Surface Science*, Vol. 258, No. 6, 2068-2076, doi: [10.1016/j.apsusc.2011.04.064](https://doi.org/10.1016/j.apsusc.2011.04.064).
- [14] Yasavol, N., Abdollah-zadeh, A., Ganjali, M., Alidokht, S.A. (2013). Microstructure and mechanical behavior of pulsed laser surface melted AISI D2 cold work tool steel, *Applied Surface Science*, Vol. 265, 653-662, doi: [10.1016/j.apsusc.2012.11.070](https://doi.org/10.1016/j.apsusc.2012.11.070).
- [15] Yilbas, B.S., Patel, F., Karatas, C. (2013). Laser controlled melting of HSLA steel surface with presence of B₄C particles, *Applied Surface Science*, Vol. 282, 601-606, doi: [10.1016/j.apsusc.2013.06.018](https://doi.org/10.1016/j.apsusc.2013.06.018).
- [16] Gadag, S.P., Srinivasan, M.N., Mordike, B.L. (1995). Effect of laser processing parameters on the structure of ductile iron, *Materials Science and Engineering: A*, Vol. 196, No. 1-2, 145-154, doi: [10.1016/0921-5093\(94\)09719-4](https://doi.org/10.1016/0921-5093(94)09719-4).
- [17] Vilar, R. (2014). 10.07 – Laser powder deposition, In: Hashmi, S. (ed.), *Comprehensive Materials Processing*, Vol. 10, Elsevier, 163-216, doi: [10.1016/B978-0-08-096532-1.01005-0](https://doi.org/10.1016/B978-0-08-096532-1.01005-0).
- [18] Uematsu, Y., Kakiuchi, T., Tokaji, K., Nishigaki, K., Ogasawara, M. (2013). Effects of shot peening on fatigue behavior in high speed steel and cast iron with spheroidal vanadium carbides dispersed within martensitic-matrix microstructure, *Materials Science and Engineering: A*, Vol. 561, 386-93, doi: [10.1016/j.msea.2012.10.045](https://doi.org/10.1016/j.msea.2012.10.045).
- [19] Pierson, H.O. (1996). *Handbook of refractory carbides and nitrides: properties, characteristics, processing and applications*, New Jersey, Noyes publications, USA.
- [20] Li, Y., Li, G., Yang, D., Li, G. (2012). Microstructure evolution and mechanical properties in VC/SiC nanomulti-layers, *Applied Surface Science*, Vol. 258, No. 24, 9856-9858, doi: [10.1016/j.apsusc.2012.06.042](https://doi.org/10.1016/j.apsusc.2012.06.042).
- [21] Tjong, S.C., Haydn, C. (2004). Nanocrystalline materials and coatings, *Materials Science and Engineering: R: Reports*, Vol. 45, No. 1-2, 1-88, doi: [10.1016/j.mser.2004.07.001](https://doi.org/10.1016/j.mser.2004.07.001).
- [22] Lugscheider, E., Knotek, O., Bobzin, K., Bärwulf, S. (2000). Tribological properties, phase generation and high temperature phase stability of tungsten- and vanadium-oxides deposited by reactive MSIP-PVD process for innovative lubrication applications, *Surface and Coatings Technology*, Vol. 133-134, 362-368, doi: [10.1016/S0257-8972\(00\)00963-4](https://doi.org/10.1016/S0257-8972(00)00963-4).
- [23] Frykholm, R., Andrén, H.-O. (2001). Development of the microstructure during gradient sintering of a cemented carbide, *Materials Chemistry and Physics*, Vol. 67, No. 1-3, 203-208, doi: [10.1016/S0254-0584\(00\)00440-5](https://doi.org/10.1016/S0254-0584(00)00440-5).
- [24] Ye, F., Hojamberdiev, M., Xu, Y., Zhong, L., Zhao, N., Li, Y., Huang, X. (2013). Microstructure, microhardness and wear resistance of VC_p/Fe surface composites fabricated in situ, *Applied Surface Science*, Vol. 280, 297-303, doi: [10.1016/j.apsusc.2013.04.152](https://doi.org/10.1016/j.apsusc.2013.04.152).
- [25] Hashe, N.G., Neethling, J.H., Berndt, P.R., Andrén, H.-O., Norgren, S. (2007). A comparison of the microstructures of WC-VC-TiC-Co and WC-VC-Co cemented carbides, *International Journal of Refractory Metals and Hard Materials*, Vol. 25, No. 3, 207-21, doi: [10.1016/j.ijrmhm.2006.05.001](https://doi.org/10.1016/j.ijrmhm.2006.05.001).
- [26] Kaç, S., Kusiński, J. (2003). SEM and TEM microstructural investigation of high-speed tool steel after laser melting, *Materials Chemistry and Physics*, Vol. 81, No. 2-3, 510-512, doi: [10.1016/S0254-0584\(03\)00062-2](https://doi.org/10.1016/S0254-0584(03)00062-2).